China Geology 1 (2021) 67−76

China Geology

Journal homepage: http://chinageology.cgs.cn
https://www.sciencedirect.com/journal/china-geology

Early Cretaceous deformation in the southern Tashkorgan region: Implications for the tectonic evolution of the northeastern Pamir

Zhi-hui Cai[a,*], Bi-zhu He[a], Guang-wei Li[b], Cun-li Jiao[c], Xiao-rui Yun[a]

[a] *Key Laboratory of Deep-Earth Dynamics of Ministry of Natural Resources, Institute of Geology, Chinese Academy of Geological Sciences, Beijing* 100037, *China*
[b] *State Key Laboratory for Mineral Deposits Research, School of Earth Science and Engineering, Nanjing University, Nanjing* 210046, *China*
[c] *Exploration and Production Research Institute of SINOPEC, Beijing* 100083, *China*

ARTICLE INFO

Article history:
Received 18 January 2021
Received in revised form 3 March 2021
Accepted 5 March 2021
Available online 12 March 2021

Keywords:
Early Cretaceous
Deformation
Biotite ^{40}Ar-^{39}Ar
Tashkorgan
Neo-tethyan
Pamir
Tibetan Plateau

ABSTRACT

The Pamir Plateau comprises a series of crustal fragments that successively accreted to the Eurasian margin preceded the India-Asia collision, is an ideal place to study the Mesozoic tectonics. The authors investigate the southern Tashkorgan area, northeastern Pamir Plateau, where Mesozoic metamorphic and igneous rocks are exposed. New structural and biotite ^{40}Ar-^{39}Ar age data are presented. Two stages of intense deformation in the metamorphic rocks are identified, which are unconformably covered by the Early Cretaceous sediment. Two high-grade metamorphic rocks yielding 128.4 ± 0.8 Ma and 144.5 ± 0.9 Ma ^{40}Ar-^{39}Ar ages indicate that the samples experienced an Early Cretaceous cooling event. Combined with previous studies, it is proposed that the Early Cretaceous tectonic records in the southern Tashkorgan region are associated with Andean-style orogenesis. They are the results of the flat/low-angle subduction of the Neotethyan oceanic lithosphere.

1. Introduction

The Pamir Plateau appears as a high-elevation and high-relief mountain. Similar to the Tibetan Plateau, the Pamir Plateau is a complex assemblage of multiple terranes which accreted to the southern margin of the ancient Asian continent preceded the India-Asia collision (Tapponnier P et al., 1986, 2001; Allégre CJ et al., 1984; Burtman VS and Molnar P, 1993; Yin A and Harrison TM, 2000). It is contiguous with the Tibetan Plateau to the east and is separated from the Tibetan Plateau by the Kashgar-Yecheng, Karakax and Karakorum fault systems (Cowgill E, 2010), and can be divided into North Pamir, Central Pamir, South Pamir, and Kohistan-Ladakh terranes separated by Tanymas, Rusha-Pshart, and Shyok suture zones (Fig. 1) (Burtman VS and Molnar P, 1993; Robinson AC et al., 2004, 2007, 2012, 2015; Schmidt J et al., 2011; Stübner K et al., 2013a, 2013b; Rutte D et al., 2017a, 2017b).

The Tashkorgan area of Xinjiang is located in the northeast of the Pamir Plateau. Many studies are focus on the Cenozoic tectonics of the northeastern Pamir. The Cenozoic Karakoram strike-slip fault with large scale has been argued by researchers for years (Tapponnier P et al., 1986, 2001; Searle MP et al., 1987, 1998; Lacassin R et al., 2004; Phillips RJ et al., 2004; Amidon WH and Hynek SA, 2010; Leloup PH et al., 2011). These researchers have discussed its scale, strike-slip displacement, formation time, and its contribution to the lateral extrusion of the continent after the India-Asia collision. Some researchers believe that its strike-slip reaches 1000 km or more than 400 km, which is a major channel for the eastward extrusion of Pamir materials after the India-Asia continental collision (Tapponnier P et al., 1986; Lacassin R et al., 2004; Schwab M et al., 2004). Some scholars believe that its strike-slip is much smaller and its contribution to the eastward extrusion of material is limited (Murphy MA et al., 2000; Robinson AC et al., 2009). The main viewpoint on the formation age of the dextral strike-slip fault in the Karakoram is that it occurred at Oligocene to early Miocene (Lacassin R et al. 2004; Schmalholz M et al., 2004; Valli F et al., 2007; Robinson AC et al., 2009; Amidon WH and Hynek SA, 2010; Leloup PH et al., 2011). The Cenozoic Kongur Shan Extensional Fault System in northeastern Pamir (Brunel M et al., 1994; Robinson AC et al., 2004, 2007, 2012) is also well

* Corresponding author: *E-mail address*: cai-zhihui@hotmail.com (Zhi-hui Cai).

doi:10.31035/cg2021023
2096-5192/© 2021 China Geology Editorial Office.

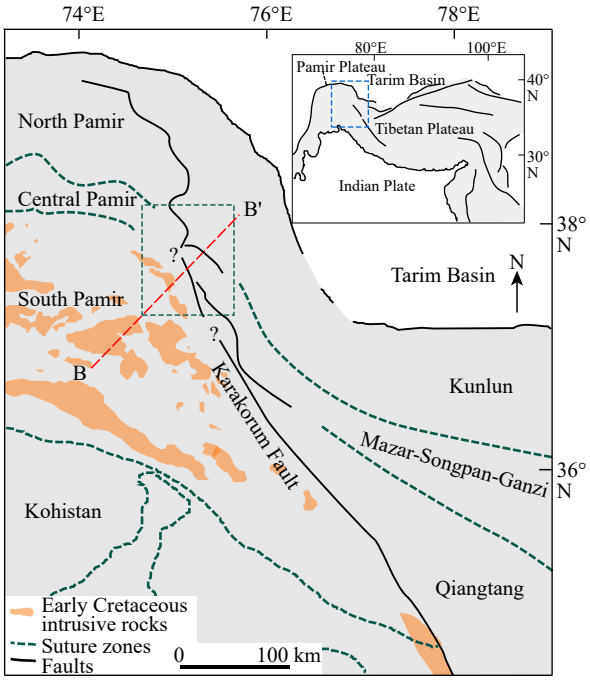

Fig. 1. Simplified geological map of the Pamir Plateau (after Robinson AC, 2009).

known and is thought to have a significant E-W extension, and began to active at Miocene (Robinson AC et al., 2007). Some studies (Robinson AC et al., 2004, 2007, 2009, 2012; Cao K et al., 2013; Cai ZH et al., 2017) are also focus on the Cenozoic gneiss domes in the northeastern Pamir. The researchers regard the Kongur Shan and Muztaghata gneiss domes underwent high-grade metamorphism (Robinson AC et al., 2004, 2007) and continued exhumation to the middle-upper crust until Miocene (Cai ZH et al., 2017). In the Pliocene-Quaternary, the gneiss domes experienced rapid exhumation (Cao K et al., 2013).

The magmatic rocks in the northeastern Pamir are also well studied. The 12 Ma to 10 Ma potassic intrusions (Robinson AC et al., 2007; Jiang YH et al., 2012) have been interpreted to be associated with the Miocene decompression melting and asthenosphere upwelling (Jiang YH et al., 2012).

The above studies have primarily concentrated on the Cenozoic tectonics in the northeastern Pamir, and relatively little attention has been paid to the Mesozoic history. Some Zircon U-Pb geochronologic, geochemical, and isotopic data for Mesozoic igneous rocks were gained to argue the magma sources and tectonic settings. The Triassic to Early Jurassic igneous rocks were regarded to be related to the subduction and closure of the Paleo-Tethys Ocean (Jiang YH et al., 2013; Liu XQ et al., 2020a). The Early Cretaceous igneous rocks were interpreted to reflect northward directed subduction of the Neo-Tethyan oceanic lithosphere (Jiang YH et al., 2014; Li J et al., 2016; Liu XQ et al., 2020b). Despite these achievements on the Mesozoic magmatic history of northeastern Pamir, rare structural data were reported in this area. This hampers the understanding of the framework of the northeastern Pamir preceded the India-Asia collision.

This paper aims to demonstrate the Early Cretaceous tectonic history of the southern Tashkorgan region, northeastern Pamir. The authors report the structural and ^{40}Ar-^{39}Ar geochronology data combining with previous studies, to serve to improve the understanding of the Mesozoic tectonics of the Tibet-Pamir Plateau.

2. Geological setting

The Tashkorgan region of Xinjiang Uggur Autonomous Region is located in the northeastern Pamir Plateau. It is the only segment of China that belongs to the Pamir Plateau. According to characteristics of the lithology and fault distribution, the Tashkorgan region can be divided into several terranes: The South Tarim, the West Kunlun, the Tashkorgan, and the Mingtiegai terranes (Wang SY and Peng SM, 2014). The southern Tashkorgan region is located in the south of the Tashkorgan Terrane. It is surrounded by the Taesi Fault to the west, Wachia Fault to the east, and Bandier Fault to the north (Fig. 2). Its north is adjacent to the Muztaghata Gneiss Dome (Robinson AC et al., 2004, 2007, 2012; Cao K et al., 2013; Cai ZH et al., 2017).

The basement in the southern Tashkorgan region is composed of two parts. The lower part is high-grade metamorphic rocks: Amphibolite, quartzite, marble, and schist bearing metamorphic minerals such as garnet and sillimanite. The upper part is Ordovician–Silurian light metamorphic sedimentary rocks (Wang SY and Peng SM, 2014; Fig. 3). The high-grade metamorphic rocks in the southern Tashkorgan region are in contact with the Ordovician–Silurian sedimentary rocks with faults (Fig. 3). The Ordovician–Silurian rocks are also slightly metamorphic, comprising siltstone, slate, crystalline limestone, meta-sandstone, and meta-volcanic rocks (Fig. 3) formed in the active continental margin environment. The Carboniferous contains mudstones, sandstones, silicalites, limestones, and few volcanic rocks (Pan YS et al., 1992; Wang JP, 2008). The Lower Cretaceous conglomerates unconformably cover the Carboniferous and Bulunkole Group (Pan YS et al., 1992; Wang JP, 2008; Fig. 3).

Based on the above lithology description, the southern Tashkorgan and other northern Pamir regions have been interpreted as having a similar basement to the North and South Kunlun Terranes in the Tibet Plateau (Burtman VS and Molnar P, 1993). Alternatively, according to detrital zircon and Sr-Nd isotopic analyses, Robinson AC et al. (2012) proposed that the medium to high-grade metamorphic rocks in the southern Tashkorgan region is Permian–Triassic in age. It belongs to the Permian –Triassic Karakul-Mazar arc-accretionary complex terrane. These different interpretations highlight the uncertainty in terrane affiliation of the southern Tashkorgan region.

3. Structural geology of the southern Tashkorgan Region

In the southern Tashkorgan region, the Lower Cretaceous Xialafdi Group unconformably overlies the Bulunkole Group (Fig. 4a) and is composed of ca. 546 m thick lacustrine delta deposits, including yellow-gray-brown conglomerates, sandstones, and limestones (Wang SY and Peng SM, 2014).

The Bulunkole Group is significantly deformed for the folds and intense foliations (Figs. 4a, b). It indicates that the ductile deformation of the Bulunkole Group occurred before the deposition age of the Xialafdi Group (Early Cretaceous).

In the southern Tashkorgan region, two stages of deformation recorded in the Bulunkole Group were recognized. The authors name them D1 and D2 as the first and second stages of deformation, respectively. The D2 is much more prominent than the D1. It overprints the D1 in most locations. The D2 foliations are continuous and generally NW-SE striking with moderate or shallow W/SW dip angle (Figs. 4a, b). The D2 stretching lineations are SW, SSW or W plunging (Figs. 4c–e), indicating a high strain rate of simple shearing. The σ-type porphyroblasts systems (Figs. 4f, g), mica fish, S-C/C' structures in the mylonites show a top-to-the-east or northeast shear sense of D2 deformation. In some locations, the D2 foliations dip to the east (Figs. 4a–h), reflecting isoclinal folding deformation. Small scale D2 folds also can be found in the field with axial surface moderately dipping to west/southwest and tight (Fig. 4h).

Within the Bulunkole Group, few relicts of the D1 structure can be identified (Figs. 4h–l). In some locations where the original bedding of the sedimentary rocks is quite thick, the D1 foliation appears as parallel to the bedding (Fig. 4i),

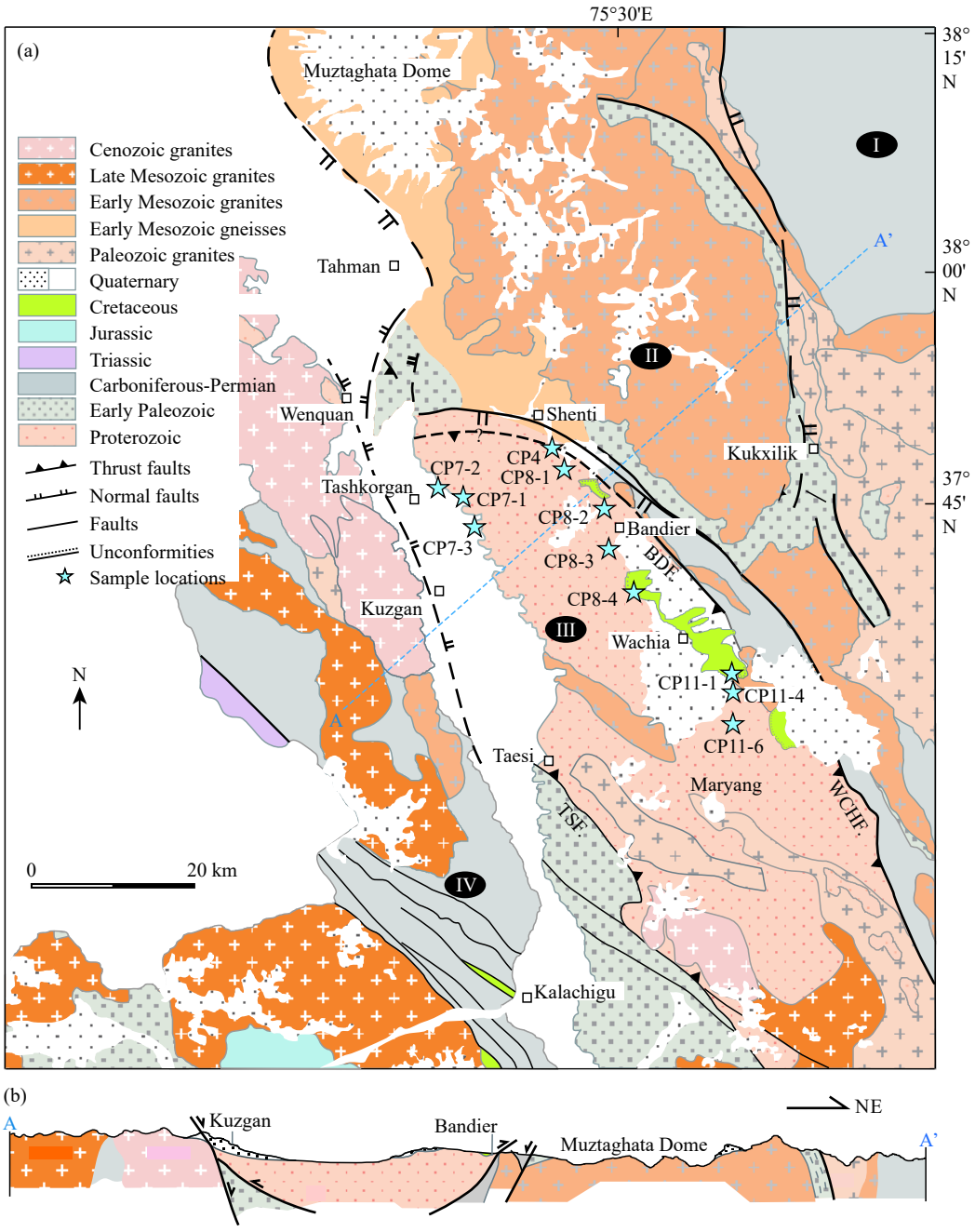

Fig. 2. a–Simplified geological map of the Tashkorgan region, northeastern Pamir (after Wang SY and Peng SM, 2014); b–cross-section across the southern Tashkorgan region (see A-A' in the Fig. 2a). I–South Tarim Terrane; II–West Kunlun Terrane; III–Tashkorgan; IV–Mingtiegai terranes. BDF–Bankier Fault; WCHF–Wachia Fualt; TSF–Taesi Fault.

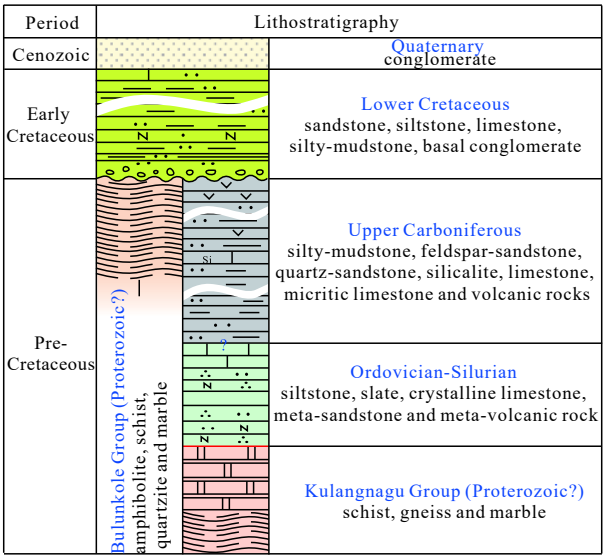

Fig. 3. Simplified stratigraphic column of the southern Tashkorgan region.

dipping to the east with a gentle angle (Fig. 4i). Immediately east of Tashkoran, remnant D1 folds were recognized. The axial surfaces of the D1 folds are mainly west-dipping and observed to rotate influenced by D2 shearing (Fig. 4j). Leucosomes, without foliation, intruded into the D1 folds, and some of them cut across the layers in the folds (Fig. 4j). The leucosomes are named MA2 leuocosomes here. In some locations, where the MA2 leuocosomes appear as thick sills or pluton, the D1 foliations can be easily observed generally dipping to SSW/W, for the D2 cutting across the D1 foliations (Figs. 4k–l).

The microstructures of mylonitic samples from the studied area are shown in Fig. 5. The foliations are defined by quartz, feldspar, biotite, muscovite, amphibole, pyroxene, sillimanite, kyanite, and et al. The mica-fish (Figs. 5a, f), σ-type garnet porphyroblasts (Figs. 5b–e), quartz shear bands, C-type (Fig. 5c), and C ’-type (Figs. 5b, f) shear bands show the latest simple shearing with a sense top-to-east or E or NE consistent with the field observations. Strongly elongated quartz ribbons with subgrains indicate a subgrain rotation recrystallization happened during the deformation. The authors regard the above deformation characteristics belong to the prominent D2. The D1 is significantly overprinted by the D2 in these samples. From the minerals (sillimanite, garnets, biotite, and recrystallized quartz) along the foliations, the D1 can be recognized (Figs. 5a–f). That means the D1 is mainly manifested as foliation defined by high-grade metamorphic minerals. The deformation occurred under a high-temperature condition. Differently, the D2 deformation could occur under hydrated conditions of medium temperature, which can be inferred from the deformed sillimanite and biotite (Tullis J, 2002). The garnet porphyroblasts, surrounded by the quartz-mica matrix, show grown over a secondary straight foliation. The matrix deformation did not affect the shapes and inclusion patterns in the porphyroblasts, indicating an inter-tectonic porphyroblast growth (Passchier CW and Trouw RAJ, 2005). The foliation in the garnet porphyroblast (pre-D1) formed earlier than the matrix foliation (D1).

The MA2 leuocosomes, cutting across the D1 foliation, are coarse-medium-grained, consist of feldspar, quartz, muscovite, and garnet, and without ductile deformed features (Figs. 4k–l).

4. ^{40}Ar-^{39}Ar geochronologic analyses and interpretation

4.1. Sample description and methods

Application of ^{40}Ar-^{39}Ar methods provides constraints on the timing of deformation and metamorphism within the southern Tashkorgan Region. Two representative high-grade schist samples were collected from the southern Tashkorgan region for biotite ^{40}Ar-^{39}Ar analyses. Sample CP7-1-10 (schist assemblage includes quartz, biotite, sillimanite, and garnet) was collected from east of Tashkorgan city. Sample CP8-2-7 (schist assemblage includes quartz, biotite, sillimanite, garnet, and kyanite) was collected from Bandier village.

Biotite grains from metasedimentary samples were separated using conventional techniques, subsequently, were sent into the nuclear reactor at the Chinese Institute of Atomic Energy in Beijing to irradiate for 1440 minutes and cooled for three months. Argon isotope analyses were conducted on an MM-1200B mass spectrometer in the Laboratory of Institute of Geology, Chinese Academy of Geological Science. Biotite grains (32.62 mg from CP7-1-10, 32.26 mg from CP8-2-7) were step-heated for ^{40}Ar-^{39}Ar analysis. The ^{40}Ar-^{39}Ar analytical data are summarized in Table 1, presented in Fig. 6. The analytical methods and age calculations are given in Chen W et al. (2006) and Zhang Y et al. (2006).

4.2. Analytical results

Fig. 6 shows ^{40}Ar-^{39}Ar step heating results for biotites from studied samples. Biotites from the two samples yielded disturbed spectrums, but with a reasonably concordant average age. The discordance in the age spectrum could because of Ar loss, different sized grains, or alteration around the biotite grain margins. The CP7-1-10 sample yielded a weighted ^{40}Ar-^{39}Ar plateau age of 128.4 ± 0.8 Ma (MSWD = 0.65; from 860°C to 1230°C, Fig. 6a). The CP8-2-7 Sample gave a ^{40}Ar-^{39}Ar plateau age of 144.5 ± 0.9 Ma (MSWD = 0.83; from 900°C to 1200°C, Fig. 6b).

5. Discussion

5.1. Timing of the deformation stages

Closure temperatures of argon are assumed to be around 300°C for biotite (Harrison TM et al., 1985), with an uncertainty of ± 50°C on closure temperatures (due to compositional and dimensional effects on diffusion parameters) (Renne PR et al., 1993). The ^{40}Ar-^{39}Ar geochronologic data in this study indicate an Early Cretaceous cooling and exhumation occurred in the southern Tashkorgan

region. The southern Tashkorgan region cooled through ca. 300°C at around 144.5–128.4 Ma.

The D1 deformation appears as foliation and folds in high-grade metamorphic rocks (Figs. 4j–l). According to the unpublished zircon and monazite U-Pb data, the metamorphism age of the high-grade schists is ca. 200 Ma

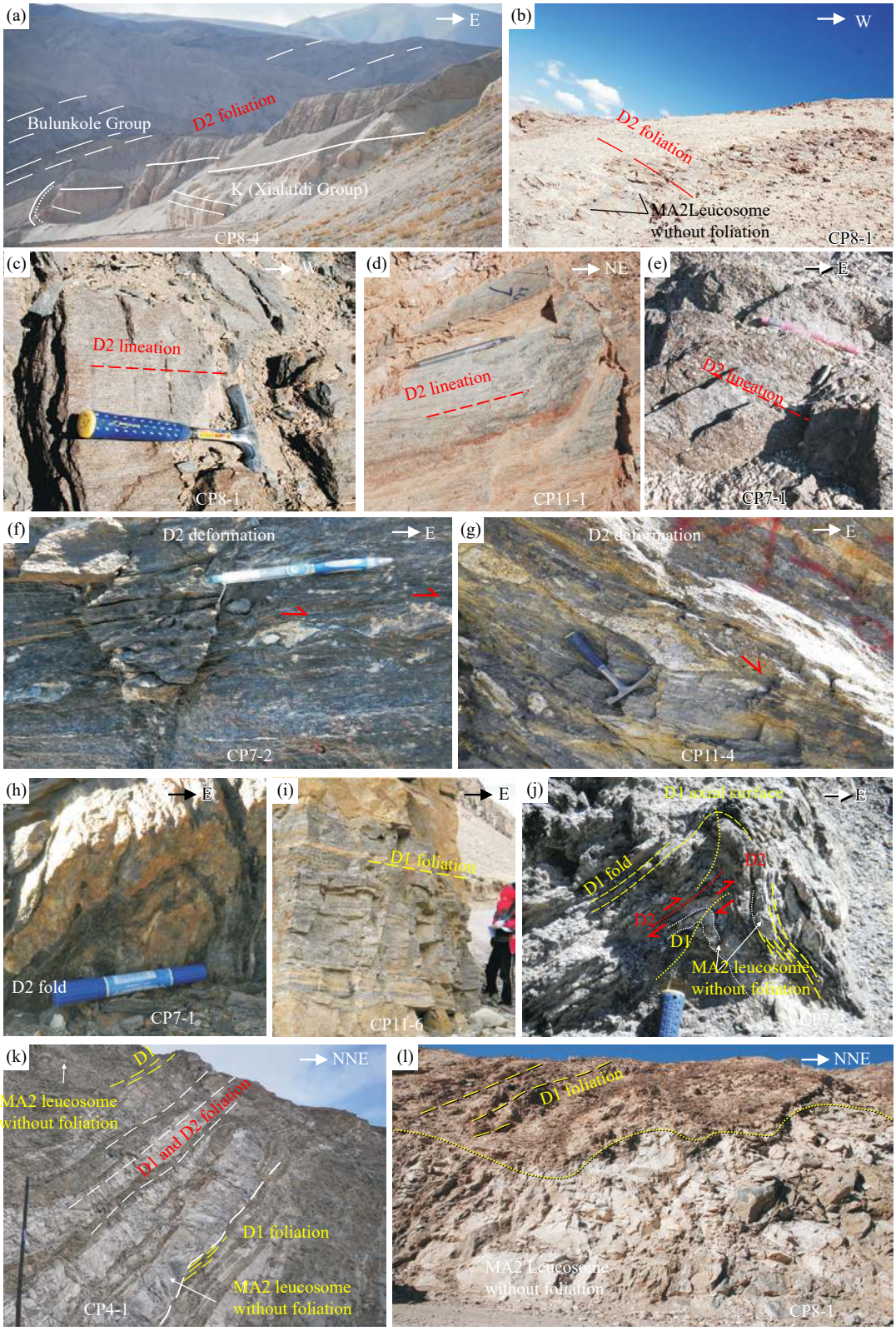

Fig. 4. Outcrop photos in the southern Tashkorgan region. a–Lower Cretaceous Xialafdi Group unconformably overlies Bulunkole Group; b–D2 foliations in schist are continuous and generally NW-SE striking with moderate or shallow W/SW dip angle; c–e–D2 stretching lineations are SW, SSW or W plunging; f, g–σ-type porphyroblasts systems in schists show a top-to-the-east or northeast sense of shear; h–D2 fold (schist); i–D1 foliation appears as parallel to the bedding; j–D1 fold is cut across by the MA2 Leucosomes; k–undeformed MA2 leucosomes with sill shape; l–undeformed MA2 leucosome pluton, cutting across the D1 foliations.

(Early Jurassic). This age constrains the D1 deformation, reflecting a primary homogeneous crust shortening and thickening.

The MA2 leuocosomes formed accompanied the D2 deformation. According to the unpublished zircon U-Pb analyses of the MA2 leuocosomes, MA2 leuocosomes crystalized at ca. 160 Ma. Herein, the D2 occurred at ca. 160 Ma, followed 144–128 Ma cooling event (this study).

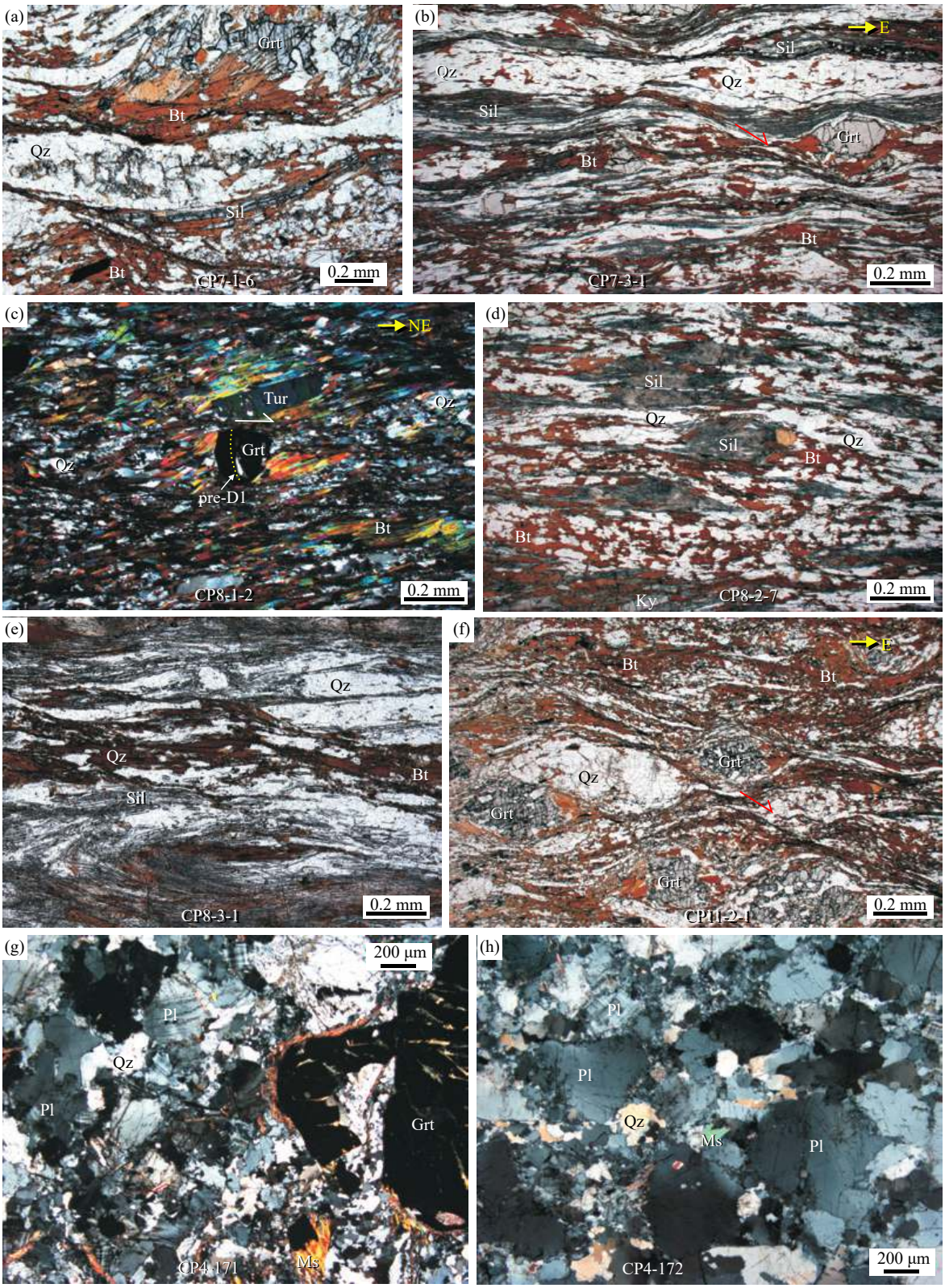

Fig. 5. Thin section photomicrographs of lithology and micro-tectonics. a–f–schist; g, h–leuocosome. Ky–kyanite, Grt–garnet, Ms–muscovite, Pl–plagioclase, Qz–quartz, Sil–Sillimanite, Tur–tourmaline, Bt–Biotite. a, b, d, e and f are under plane polarized light, and c, g and h are under crossed polarized light. Sample locations are shown in Fig. 2a.

5.2. Early Cretaceous deformation in the southern Tashkorgan region

The Early Cretaceous D2 is mainly manifested as top-to-east shearing, tight and upright folding (Figs. 4, 5), indicating an eastward décollement-like structure existed in the middle crust. This structure is proposed to be similar to the décollement in the Songpan-Garze Orogenic Belt of China (Xu ZQ et al., 1992). It always occurs between the crystalline basement and sedimentary cover under a crustal shortening regime.

Intensely deformed Bulunkole Group is unconformably underlined by the conglomerates in the Lower Cretaceous

Table 1. Ar-Ar dating results for the samples from southern Tashkorgan region.

T/°C	$(^{40}Ar/^{39}Ar)_m$	$(^{36}Ar/^{39}Ar)_m$	$(^{37}Ar_0/^{39}Ar)_m$	$(^{38}Ar/^{39}Ar)_m$	F	$^{39}Ar/^{-14}mol$	Apparent age/Ma	±2σ/Ma
CP7-1-10 Biotite, W = 32.62 mg, J = 0.003468								
Total age = 128.6 Ma; 86 – 1230°C WMPA = 128.4 ± 0.8 Ma, MSWD = 0.65								
700	245.4229	0.7303	0.0000	0.1151	29.6069	0.01	176.0	47.0
800	52.1743	0.1209	0.4670	0.0342	16.4827	0.13	100.3	3.6
860	29.3297	0.0279	0.0921	0.0181	21.0977	2.33	127.4	1.2
900	22.6913	0.0048	0.0320	0.0136	21.2632	7.81	128.4	1.2
940	21.9491	0.0019	0.0274	0.0130	21.3970	2.76	129.1	1.3
980	21.8960	0.0016	0.0344	0.0131	21.4253	4.92	129.3	1.3
1020	21.8804	0.0028	0.3192	0.0136	21.0677	1.53	127.2	1.3
1060	21.9127	0.0031	0.2642	0.0134	21.0127	1.20	126.9	1.3
1100	21.9053	0.0027	0.3744	0.0135	21.1343	1.52	127.6	1.3
1140	21.8648	0.0017	0.0717	0.0130	21.3710	3.73	129.0	1.2
1180	22.2091	0.0026	0.0091	0.0132	21.4478	4.74	129.4	1.3
1230	22.3636	0.0029	0.0000	0.0130	21.5024	4.61	129.7	1.3
1300	23.1777	0.0100	2.3748	0.0173	20.4284	0.24	123.5	1.7
1400	34.3942	0.0585	3.1271	0.0054	17.3623	0.03	105.5	9.1
CP8-2-7 Biotite, W = 32.26 mg, J = 0.003397								
Total age = 144.7 Ma; 900 – 1200°C, WMPA = 144.5 ± 0.9 Ma, MSWD = 0.83								
700	58.7124	0.1652	0.0000	0.0453	9.8778	0.04	60.0	11.0
800	38.8612	0.0733	1.1515	0.0313	17.2988	0.14	103.0	2.2
860	37.3467	0.0497	0.2422	0.0238	22.6688	1.61	133.8	1.3
900	27.1498	0.0101	0.0000	0.0157	24.1752	4.15	142.4	1.4
940	25.3830	0.0027	0.0000	0.0142	24.5761	3.31	144.6	1.4
980	25.2100	0.0018	0.0000	0.0138	24.6605	2.31	145.1	1.4
1020	25.3370	0.0019	0.0000	0.0138	24.7629	1.53	145.7	1.4
1070	25.1289	0.0020	0.0741	0.0142	24.5377	1.67	144.4	1.4
1120	24.9489	0.0022	0.0610	0.0144	24.2930	3.02	143.0	1.4
1160	25.0148	0.0012	0.0000	0.0140	24.6515	6.13	145.1	1.4
1200	25.1243	0.0010	0.0111	0.0140	24.8241	5.64	146.1	1.4
1240	25.2439	0.0001	0.0316	0.0139	25.2076	7.03	148.2	1.4
1280	25.7244	0.0015	0.0000	0.0140	25.2907	1.09	148.7	1.5
1400	47.9704	0.0258	8.9169	0.0258	41.2568	0.02	237.0	27.0
1300	18.1193	0.0496	0.0000	0.0274	19.1300	0.15	14.1	1.4

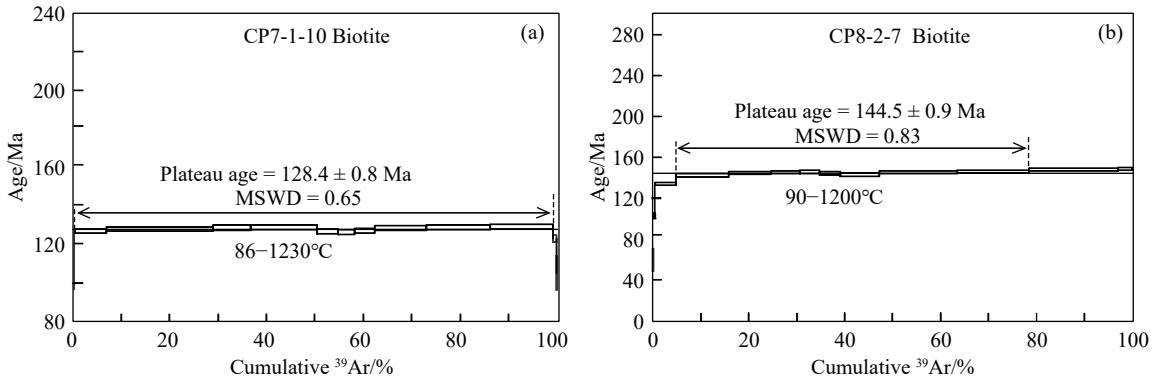

Fig. 6. ^{40}Ar-^{39}Ar age spectras of biotites in the southern Tashkorgan region.

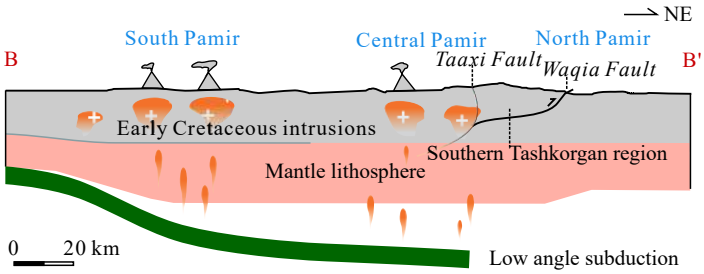

Fig. 7. Early Cretaceous synthetic cross-sections of the tectonic model in the northeastern Pamir (see B-B' in the Fig. 1).

Xialafdi Group (Fig. 4a) combining with the Early Cretaceous biotite ^{40}Ar-^{39}Ar cooling ages (144 –128 Ma) reflect the exhumation process in the southern Tashkorgan region. It means, from 144 –128 Ma to the deposition time of the Xialafdi Group (Lower Cretaceous), the deformed Bulunkole Group rapidly exhumed from the middle crust to the surface.

5.3. Tectonic implications

Before this study, Cretaceous ^{40}Ar-^{39}Ar cooling ages and Cretaceous amphibolite facies metamorphism in the northeastern Pamir have been reported by Robinson AC et al. (2007, 2015). Additionally, Early Cretaceous igneous rocks are widely distributed in the northern Pamir (Jiang YH et al., 2014; Li J et al., 2016; Chapman JB et al., 2018b; Liu XQ et al., 2020b). Combined these data with the structural and ^{40}Ar-^{39}Ar data in this study, the Early Cretaceous tectonism of the northeastern Pamir can be proposed to be including magmatism, significant shortening and exhumation.

The authors explain the Early Cretaceous magmatism, shortening and exhumation in the northeastern Pamir are results of the low-angle to flat subduction and roll-back of the Neotethyan oceanic slab. The northern and southern Pamir regions are far from the subduction zone of the Shyok oceanic lithosphere (Neothys), which was subducting northward during the Cretaceous. To form the Cretaceous magmatism (Searle MP et al., 1987, 2010; Schwab M et al., 2004; Chapman JB et al., 2018b; Liu XQ et al., 2020b) and crustal thickening (this paper), a low-angle to flat subduction is required, which can well explain the intracontinental deformation inland far from the trench (Jordan TE et al., 1983; Fig. 7). The exhumation of the high-grade metamorphic rocks in the northeastern Pamir might be due to the roll-back of the Neotethyan oceanic slab (Chapman JB et al., 2018a).

6. Conclusions

(i) The authors recognize two intense deformational records in the high-grade metamorphic rocks and relate them to the Early Jurassic to Early Cretaceous tectonic evolution of the southern Tashkorgan region.

(ii) The high-grade metasedimentary rocks in the southern Tashkorgan region record Early Cretaceous cooling ages of 144.5 ± 0.9 Ma and 128.4 ± 0.8 Ma, indicating an Early Cretaceous exhumation.

(iii) The Early Cretaceous magmatism, exhumation, and sedimentary records imply Andean-style orogenesis occurred.

(iv) The Early Cretaceous crustal deformation of the northeastern Pamir may be occurred by low-angle subduction of the Neotethyan oceanic lithosphere.

CRediT authorship contribution statement

Zhi-hui Cai conceived of the presented idea. Zhi-hui Cai, Bi-zhu He, Cun-li Jiao and Xiao-rui Yun carried out the field work and supervised the findings of this work. Zhi-hui Cai and Xiao-rui Yun carried out the experiments. Zhi-hui Cai, Bi-zhu He and Guang-wei Li contributed to the interpretation of the results. Zhi-hui Cai took the lead in writing the manuscript. All authors discussed the results and contributed to the final manuscript.

Declaration of competing interest

The authors declare no conflicts of interest.

Acknowledgment

Dong-liang Liu and Wei-feng Xiao are acknowledged for giving suggestions and improving the paper. Zuo-lin Tian is acknowledged for the discussion. This work is supported by the National Natural Science Foundation of China (91955203, 91755101, 41872121, 41302166), the fund from the Key Laboratory of Deep-Earth Dynamics of Ministry of Natural Resources (J1901-20-4), Scientific Research Fund of the Institute of Geology, Chinese Academy of Geological Sciences (S2003), the Basic Research Project of Chinese Academy of Geological Sciences (JYYWF20180903, JYYWF20182103), and the project of China Geological Survey (DD20190006, DD20190060). All cited data are available in referenced publications.

References

Allégre CJ, Courtillot V, Tapponnier P, Hirn A, Mattauer M, Coulon C, Jaeger JJ, Achache J, Scharer U, Marcoux J, Burg JP, Girardeau J, Armijo R, Gariepy C, Gopel C, Li TD, Xiao XC, Chang CF, Li GQ, Lin BY, Teng JW, Wang NW, Chen GM, Han TL, Wang XB, Den WM, Sheng HB, Cao YG, Zhou J, Qiu HR, Bao PS, Wang SC, Wang BX, Zhou YX, Ronghua X. 1984. Structure and evolution of the Himalaya-Tibet orogenic belt. Nature, 307, 17–22. doi: 10.1038/307017a0.

Amidon WH, Hynek SA. 2010. Exhumational history of the north central Pamir. Tectonics, 29(5), 5966–5983. doi: 10.1029/2009TC002589.

Brunel M, Arnaud N, Tapponnier P, Pan Y, Wang Y. 1994. Kongur Shan normal fault: Type example of mountain building assisted by extension (Karakoram fault, eastern Pamir). Geology, 22, 707–710. doi: 10.1130/0091-7613(1994)022<0707:KSNFTE>2.3.CO;2.

Burtman VS, Molnar P. 1993. Geological and geophysical evidence for deep subduction of continental crust beneath the Pamir. Speccial Paper of America Geological Society, 281, 1–76. doi: 10.1130/SPE281-p1.

Cai ZH, Xu ZQ, Cao H, Robinson AC, Li GW, Xu XY. 2017. Miocene exhumation of northeast Pamir: Deformation and geo/thermochronological evidence from western Muztaghata shear zone and Kuke ductile shear zone. Journal of Structural Geology, 102, 130–146. doi: 10.1016/j.jsg.2017.07.010.

Cao K, Bernet M, Wang GC, van der Beek P, Wang A, Zhang KX, Enkelmann E. 2013. Focused Pliocene –Quaternary exhumation of the Eastern Pamir domes, western China. Earth and Planetary Science Letters, 363(2), 16–26. doi: 10.1016/j.epsl.2012.12.023.

Chapman JB, Robinson AC, Carrapa B, Villarreal D, Worthington J, DeCelles PG, Kapp P, Gadoev M, Oimahmadov I, Gehrels G. 2018a. Cretaceous shortening and exhumation history of the South Pamir terrane. Lithosphere, 10(4), 494–511. doi: 10.1130/L691.1.

Chapman JB, Scoggin SH, Kapp P, Carrapa B, Ducea MN, Worthington J, Oimahmadov I, Gadoev M. 2018b. Mesozoic to Cenozoic magmatic history of the Pamir. Earth and Planetary Science Letters, 482, 181–192. doi: 10.1016/j.epsl.2017.10.041.

Chen W, Zhang Y, ZhangYQ, Jin GS, Wang Q. 2006. Late Cenozoic episodic uplifting in southeastern part of the Tibetan Plateu: Evidence from Ar-Ar thermochronology. Aca Petrologica Sinica, 22(4), 867–872 (in Chinese with English abstract). doi: 10.1016/j.sedgeo.2005.11.021.

Cowgill E. 2010. Cenozoic right-slip faulting along the eastern margin of the Pamir salient, northwestern China. GSA Bulletin, 122(1/2), 145–161. doi: 10.1130/B26520.1.

Harrison TM, Duncan I, McDougall I. 1985. Diffusion of ^{40}Ar in biotite: Temperature, pressure and compositional effects. Geochimica et Cosmochimica Acta, 49, 2461–2468. doi: 10.1016/0016-7037(85)90246-7.

Jiang YH, Liu Z, Jia RY, Liao SY, Zhao P, Zhou Q. 2014. Origin of Early Cretaceous high-K calc-alkaline granitoids, western Tibet: Implications for the evolution of the Tethys in NW China. International Geology Review, 56, 88–103. doi: 10.1080/01431161.2013.819963.

Jiang YH, Jia RY, Liu Z, Liao SY, Zhao P, Zhou Q. 2013. Origin of Middle Triassic high-K calc-alkaline granitoids and their potassic microgranular enclaves from the western Kunlun orogen, northwest China: A record of the closure of Paleo-Tethys. Lithos, 156 –159, 13–30. doi: 10.1016/j.lithos.2012.10.004.

Jiang YH, Liu Z, Jia RY, Liao SY, Zhou Q, Zhao P. 2012. Miocene potassic granite-syenite association in western Tibetan Plateau: Implications for shoshonitic and high Ba-Sr granite genesis. Lithos, 134–135, 146–162. doi: 10.1016/j.lithos.2011.12.012.

Jordan TE, Isacks BL, Allmendinger RW, Brewer JA, Ramos VA, Ando CJ. 1983. Andean tectonics related to geometry of subducted Nazca plate. Geological Society of America Bulletin, 94, 341–361. doi: 10.1130/0016-7606(1983)942.0.CO;2.

Lacassin R, Valli F, Arnaud N, Leloup PH, Paquette JL, Li HB, Tapponnier P, Chevalier ML, Guillot S, Maheo G, Xu ZQ. 2004. Large-scale geometry, offset and kinematic evolution of the karakorum fault, Tibet. Earth and Planetary Science Letters, 219(3–4), 255–269. doi: 10.1016/S0012-821X(04)00006-8.

Leloup PH, Boutonnet E, Davis WJ, Hattori K. 2011. Long-lasting intracontinental strike-slip faulting: New evidence from the Karakorum shear zone in the Himalayas. Terra Nova, 23(2), 92–99. doi: 10.1111/j.1365-3121.2011.00988.x.

Li J, Niu Y, Hu Y, Chen S, Zhang Y, Duan M, Sun P. 2016. Origin of the late Early Cretaceous granodiorite and associated dioritic dikes in the Hongqi-lafu pluton, northwestern Tibetan Plateau: A case for crust-mantle interaction. Lithos, 260, 300–314. doi: 10.1016/j.lithos.2016.05.028.

Liu XQ, Zhang CL, Hao XS, Zou HB, Wang Q, Hao XS, Zhao HX, Ye XT. 2020a. Triassic-Jurassic Granitoids and Pegmatites from Western Kunlun-Pamir Syntax: Implications for the Paleo-Tethys Evolution at the Northern Margin of the Tibetan Plateau. Lithosphere, 2020(1), 7282037. doi: 10.2113/2020/7282037.

Liu XQ, Zhang CL, Hao XS, Zou HB, Zhao HX, Ye XT. 2020b. Early Cretaceous granitoids in the Southern Pamir: Implications for the Meso-Tethys evolution of the Pamir Plateau. Lithos, 362 –363, 105492. doi: 10.1016/j.lithos.2020.105492.

Murphy MA, Yin A, Kapp P, Harrison TM, Ding L, Guo JH. 2000. Southward propagation of the Karakoram fault system, southwest Tibet: Timing and magnitude of slip. Geology, 28, 451–454. doi: 10.1130/0091-7613(2000)28<447:ACAFTO>2.0.CO;2.

Pan YS, Zheng D, Zhang QS. 1992. Introduction to Integrated Scientific Investigation on Karakorum and Kunlun Mountains. Beijing, China Meteorological Press, 91. (in Chinese)

Passchier CW, Trouw RAJ. 2005. Microtectonics. Second edition. Berlin, Springer, 352.

Phillips RJ, Parrish RR, Searle MP. 2004. Age constraints on ductile deformation and long-term slip rates along the Karakoram fault zone, Ladakh. Earth and Planetary Science Letters, 226(3 –4), 305–319. doi: 10.1016/j.epsl.2004.07.037.

Renne PR, Tobisch OT, Saleeby JB. 1993. Thermochronologic record of pluton emplacement, deformation, and exhumation at Courtright shear zone, central Sierra Nevada, Renne PR, Tobisch OT, Saleeby JB. Thermochronologic record of pluton emplacement, deformation, and exhumation at Courtright shear zone, central Sierra Nevada, California. Geology, 21 (4), 331–334. https://doi.org/10.1130/0091-7613(1993)0212.3.CO;2

Robinson AC. 2015. Mesozoic tectonics of the Gondwanan terranes of the Pamir plateau. Journal of Asian Earth Sciences, 102, 170–179. doi: 10.1016/j.jseaes.2014.09.012.

Robinson AC, Ducea M, Lapen TJ. 2012. Detrital zircon and isotopic constraints on the crustal architecture and tectonic evolution of the northeastern Pamir. Tectonics, 31(2), 2016. doi: 10.1029/2011TC003013.

Robinson AC. 2009. Geologic offsets across the northern Karakorum fault: Implications for its role and terrane correlations in the western Himalayan-Tibetan orogen. Earth and Planetary Science Letters, 279, 123–130. doi: 10.1016/j.epsl.2008.12.039.

Robinson AC, Yin A, Manning CE, Harrison TM, Zhang SH, Wang XF. 2007. Cenozoic evolution of the eastern Pamir: Implications for strain-accommodation mechanisms at the western end of the Himalayan-Tibetan orogen. Geological Society of America Bulletin, 119, 882–896. doi: 10.1130/B25981.1.

Robinson AC, Yin A, Manning CE, Harrison TM, Zhang SH, Wang XF. 2004. Tectonic evolution of the northeastern Pamir: Constraints from the northern portion of the Cenozoic Kongur Shan extensional system. Geological Society of America Bulletin, 116, 953–974. doi: 10.1130/B25375.1.

Rutte D, Lothar R, Schneider S, Stübner K, Stearns MA, Gulzar MA, Hacker BR. 2017a. Building the Pamir-Tibetan Plateau-Crustal stacking, extensional collapse, and lateral extrusion in the Central Pamir: 1. Geometry and kinematics. Tectonics, 36, 342–384. doi: 10.1002/2016TC004293.

Rutte D, Ratschbacher L, Khan J, Stübner K, Hacker BR, Stearns MA, Enkel-mann E, Jonckheere R, Pfänder JA, Sperner B, Tichomirowa M. 2017b. Building the Pamir-Tibetan Plateau- Crustal stacking, extensional collapse, and lateral extrusion in the Central Pamir: 2.

Timing and rates. Tectonics, 36, 385–419. doi: 10.1002/2016TC004294.

Schmalholz M. 2004. The Amalgamation of the Pamirs and Their Subsequent Evolution in the Far Field of the India-Asia Collision. Germany, Univ.of Tübingen, Tübingen, 1 –185. https://doi.org/10.1016/j.tet.2013.05.043

Schmidt J, Hacker BR, Ratschbacher L, Stübner K, Stearns M, Kylander-Clark A, Cottle JM, Alexander A, Webb G, Gehrels G, Minaev V. 2011. Cenozoic deep crust in the Pamir. Earth and Planetary Science Letters, 312, 411–421. doi: 10.1016/j.epsl.2011.10.034.

Schwab M, Ratschbacher L, Siebel W, McWilliams M, Minaev V, Lutkov V, Chen F, Stanek K, Nelson B, Frisch W, Wooden JL. 2004. Assembly of the Pamirs: Age and origin of magmatic belts from the southern Tien Shan to the southern Pamirs and their relation to Tibet. Tectonics, 23(4), TC4002.1–TC4002.31. doi: 10.1029/2003TC001583.

Searle MP, Parrish RR, Thow AV, Noble SR, Phillips RJ, Waters DJ. 2010. Anatomy, age and evolution of a collisional mountain belt: The Baltoro granite batholith and Karakoram Metamorphic Complex, Pakistani Karakoram. Journal of Geological Society, 167, 183–202. doi: 10.1144/0016-76492009-043.

Searle MP, Weinberg RF, Dunlap WJ. 1998. Transpressional tectonics along the Karakoram fault zone, northern Ladakh: Constraints on Tibetan extrusion. Geological Society London Special Publications, 135(1), 307–326. doi: 10.1144/GSL.SP.1998.135.01.20.

Searle MP, Windley BF, Coward MP, Cooper DJW, Rex AJ, Rex D, Tingdong L, Xuchang X, Jan MQ, Thakur VC, Kumar S. 1987. The closing of Tethys and the tectonics of the Himalaya. Geological Society of America Bulletin, 98, 678–701. doi: 10.1130/0016-7606(1987)982.0.CO;2.

Stübner K, Ratschbacher L, Rutte D, Stanek K, Minaev V, Wiesinger M, Gloaguen R. 2013a. The giant Shakhdara migmatitic gneiss dome, Pamir, India-Asia collision zone: 1. Geometry and kinematics. Tectonics, 32, 948–979. doi: 10.1002/tect.20057.

Stübner K, Ratschbacher L, Weise C, Chow J, Hofmann J, Khan J, Rutte D, Sperner B, Pfänder JA, Hacker BR, Dunkl I. 2013b. The giant Shakhdara migmatitic gneiss dome, Pamir, India-Asia collision zone: 2. Timing of dome formation. Tectonics, 32, 1404–1431. doi: 10.1002/tect.20059.

Tapponnier P, Peltzer G, Armijo R. 1986. On the mechanics of the collision between India and Asia. Geological Society of America, 19, 115–157. doi: 10.1144/GSL.SP.1986.019.01.07.

Tapponnier P, Xu ZQ, Roger F, Meyer B, Arnaud N, Wittlinger G, Yang JS. 2001. Oblique stepwise rise and growth of the Tibet plateau. Science, 294(23), 1671–1677. doi: 10.1126/science.105978.

Tullis J. 2002. Deformation of granitic rocks: Experimental studies and natural examples. In: Karato S, Wenk H (Eds.). Reviews in Mineralogy and Geochemistry, Plastic Deformation of Minerals and Rocks, vol. 51. Washington, DC, The Mineralogical Society of America, 51–95. https://doi.org/10.2138/gsrmg.51.1.51

Valli F, Arnaud N, Leloup PH, Sobel ER, Mahéo G, Lacassin R, Guillot S, Li HB, Tapponnier P, Xu ZQ. 2007. Twenty million years of continuous defromation along the Karakorum fault, western Tibet: A thermochronological analysis. Tectonics, 26, TC4004. doi: 10.1029/2005TC001913.

Wang JP. 2008. Geological features and tectonic significance of melange zone in the Taxkorgan area, West Kunlun. Geological Bulletin of China, 27, 2057–2066 (in Chinese with English abstract). doi: 10.3969/j.issn.1671-2552.2008.12.011.

Wang SY, Peng SM. 2014. Regional Geological reports (1∶250000) of Keketuluke Region (J43C003002) and Tashkorgan Region (J43C003003), Wuhan, CUGP.

Xu ZQ, Hou LW, Wang ZX, Fu XF, Huang MH. 1992. Orogenic Processes of the Songpan-Garze Orogenic Belt of China. Beijing, Geological Publishing House, 190. (in Chinese)

Yin A, Harrison TM. 2000. Geologic evolution of the Himalayan-Tibetan orogen. Annual Review of Earth and Planetary Sciences, 28, 211–280. doi: 10.1146/annurev.earth.28.1.211.

Zhang Y, Chen W, Chen KL, Liu XY. 2006. Study on the Ar-Ar age spectrum of diagenetic I/S and the mechanism of ^{39}Ar recoil loss examples from the clay minerals of P-T boundary in changxing, Zhejiang province. Geological Review, 52(4), 556–561 (in Chinese with English abstract). doi: 10.1007/s11442-006-0415-5.